

*Full Length Research Paper*

# Geostatistical calculation for clay reserve in Azraq Basin in Jordan

A. Salman<sup>1\*</sup>, Khalil M. Ibrahim<sup>2</sup>, Ghazi Saffarini<sup>3</sup> and Mohammad Al-Qinna<sup>4</sup>

<sup>1</sup>Department of Geology, University of Jordan, Amman, Jordan.

<sup>2</sup>Department of Environmental and Geology, Hashemite University, Zarqa, SC 29208 Jordan.

<sup>3</sup>Department of Geology University of Jordan, Amman, SC 29208 Jordan.

<sup>4</sup>Department of Land Management and Environment, Hashemite University, Zarqa, Jordan.

Accepted 18 March, 2009

Industrial minerals in the Hashemite Kingdom of Jordan are vital to both economical and industrial development and this is true as far as the estimation of the reserves is carried out appropriately. The aim of this study was to geostatistically investigate the clay spatial behavior and geological reserve in Qa' Al-Azraq area in north east Jordan through known seventy four random drilled boreholes. Quantification of spatial arrangement or dependence was investigated through defining the best variogram model using optimal unbiased geostatistical tools of ArcGIS-Geostatistical Analyst, and MINEX. Clay thickness kriged map indicates a central concentration distribution of clay. Variations in kriged map tones comply with the major local fault systems allocated at the center of the study area forming pond structure bounded by the four faults. Two east-west cross sections were implemented using MINEX software. They provide visual maps for clay thickness distribution along the impurities of diatomite and interburden layers of silt, sand and gypsum. Clay reserves estimated using Inverse Distance Method (IDM) and Ordinary Kriging Method (OKM) were 6.1 and 5.94 Billion Cubic Meter respectively. The results of this study indicate that the area is a promising future target for economic investment in the local raw materials.

**Key words:** Ore reserve, ordinary kriging, arcmap, MINEX.

## INTRODUCTION

Industrial minerals in The Hashemite Kingdom of Jordan are vital to economical and industrial development in view of quality and adequate quantity. Thus, reserves estimation should be carried out appropriately. Among these industrial minerals are the clay deposits that are located in Qa' Al-Azraq area northeast Jordan.

Estimation of industrial minerals reserves requires a statistical tool that is optimal and unbiased. However in nature, minerals are not purely random on a landscape but have some spatial arrangement that depends on inherent and altered characteristics and therefore, classical statistical methods of analysis are not appropriate (Al-Qinna, 2003). Quantification of spatial arrangement or dependence is determined using geostatistical methods. According to the first law of geostatistics, variables that are close to each other have similar magnitudes (that is,

closely-spaced variables may be spatially correlated), whereas samples taken farther apart have values differing by a greater order of magnitude. Therefore, spatial data correlation between neighbors should be estimated and used for prediction of the overall area (Issaks and Srivastava, 1989).

Within the last 25 years, geostatistical methods have been introduced and applied to provide a best linear unbiased estimate (BLUE) of parameter values at unsampled locations. The major difference between geostatistical and classical statistics is that the former allows direct modeling of the inherent spatial data correlation (Sutherland et al., 1991; Triantafilis et al., 2001).

Geostatistical analyses imply the use of correlograms, variograms, and kriging. The correlogram is an ordered set of correlation coefficients for a common variable, where each pair of measurements is separated by distance (h). Autocorrelation is a measure of the dependency between neighboring samples.

The autocorrelation coefficient  $[\rho(h)]$  of a regionalized

\*Corresponding author. E-mail: [abeer\\_79@hotmail.com](mailto:abeer_79@hotmail.com).

variable  $Z(x)$  is defined by equation [1], where the covariance (Cov) is for any two values of  $Z$  at a distance  $h$  apart,  $C(0)$  is the variance at distance zero and  $C(h)$  is the sample covariance function defined in equation [2],

$$\rho(h) = \frac{\text{Cov}[Z(x), Z(x+h)]}{\text{variance}(Z(x))} = \frac{C(h)}{C(0)} \quad [1]$$

$$C(h) = \left[ \frac{1}{N(h)-1} \right] \times \sum [Z(x) - Z(x_e)][Z(x+h) - Z(x_e)] \quad [2]$$

where  $N(h)$  is the number of pairs of sample data taken a distance  $h$  apart (or lag) and  $Z(x_e)$  is the arithmetic mean of the data. The autocorrelation coefficient,  $\rho(h)$  is dimensionless and varies between +1 and -1 indicating perfect positive and perfect negative correlations respectively. The maximum  $\rho(h)$  occurs at zero lag ( $h = 0$ ), and the  $\rho(h)$  values tend to decrease for larger lags. Therefore, as lag distance increases, the correlation between the observations decreases (that is, covariance decreases), which indicates that samples collected close together are more alike, samples somewhat separated are less alike and samples remote from each other are not correlated at all. Eventually, for large lags or distances,  $\rho(h)$  is approximately zero and no correlation or spatial dependence exists.

For characterizing spatial correlation the semivariogram is used. The semivariogram is a graph describing the expected squared difference in value between pairs of samples with a given relative orientation where it expresses the degree of spatial variation as a function of distance (Selker et al., 1999).

Mathematically, the experimental semivariogram is computed from equation [3], where the value of  $N(h)$  depends on the number of pairs of observations used in the analysis separated by a distance or lag vector  $h$ .

$$\gamma(h) = \frac{1}{2N(h)} \sum_{i=1}^{N(h)} [(Z(x) - Z(x+h))]^2 \quad [3]$$

There are several possible mathematical functions used to model semivariograms, but only a few are commonly used (Scott, 2000).

The second step of a geostatistical analysis is kriging, which is a weighted-interpolation scheme named after D. G. Krige. Kriging provides a mean of interpolating values of points not physically sampled but using knowledge about the spatial relationships of the data set as in Equation [4]. Kriging always produces the best linear unbiased estimation (Clark, 1984).

$$Z^*(X_0) = \sum \lambda_i \gamma(x_i) \quad [4a]$$

$$\sum \lambda_i = 1 \quad [4b]$$

where  $Z^*(X_0)$  is the estimated value of  $Z$  at  $x_0$ , and  $\lambda_i$  is the weight that gives the best possible estimation from the surrounding points.

Aims of this study were to compare between geospatial modeling of geospatial programs ArcGIS Geostatistical Analyst (ESRI® version 9.0, 2004) and MINEX software (Mining software system of ECS Company, 1997) to define the spatial distributional behavior of clays in the study area using the seventy four boreholes data that were drilled by the Natural Resource Authority (NRA), and to calculate the ore reserves using advanced statistical and geostatistical techniques.

## CHARACTERIZATION OF THE STUDY AREA

The study area is located 110 km east of Amman and covers approximately an area of 370 km<sup>2</sup> that is characterized by a low relief (Figure 1). The altitude varies from 501 m (above mean sea level) in the middle of the area to 538 m in the southeastern part. Qa' Al Azraq is characterized by a dish-like basin, filled with post-Miocene lake sediments including some mineral resources. The deposits are mainly clay minerals. Khoury in (1980) indicated that the Azraq clay deposits were composed of mixed layer, montmorillonite/illite of 70% expandability where the expandable layer passes variable negative charge. The lake also deposits the sand, diatomaceous clay, carbonates, halite and gypsum (Ala'li and Abu Salah, 1993).

Seventy four boreholes were drilled in the area by the Natural Resources Authority (NRA) in 1992. They reported presence of clay deposits as the major component.

## METHODOLOGY

### Spatial analysis

The clay reserves at the seventy four boreholes were spatially investigated through detailed characterization of the autocorrelation and semivariograms components using the three geostatistical programs. Autocorrelations and correlograms were calculated and constructed using Equation [2] to explore the spatial distribution of clay on a point scale using the ArcGIS-Geostatistical analyst.

Semivariances were evaluated using the uniform interval class by calculating  $\gamma(h)$  according to equation [3] for all possible pairs of points in the data set.

Semivariogram analyses provide five types of isotropic models, each of which can be described based on three parameters: (1) nugget variance or  $C_0$ , the y-intercept of the model, (2) sill or  $C_0+C$ , the model asymptote and (3) range or  $A_0$ , the distance over which spatial dependence is apparent.

Proportions of spatial structure or  $C/(C_0+C)$  were calculated. This statistic provides a measure of the proportion of sample variance ( $C_0+C$ ) that is explained by spatially structured variance  $C$ . The coefficient of determination  $R^2$ , provides an indication of how well the model fits the variogram data. This statistical parameter is not as sensitive or robust as the residual sums of squares (RSS) for best-fit calculations. Residual sums of squares provide an exact measure of how well the model fits the variogram data. The lower the reduced sums of squares, the better the model fits the data. At

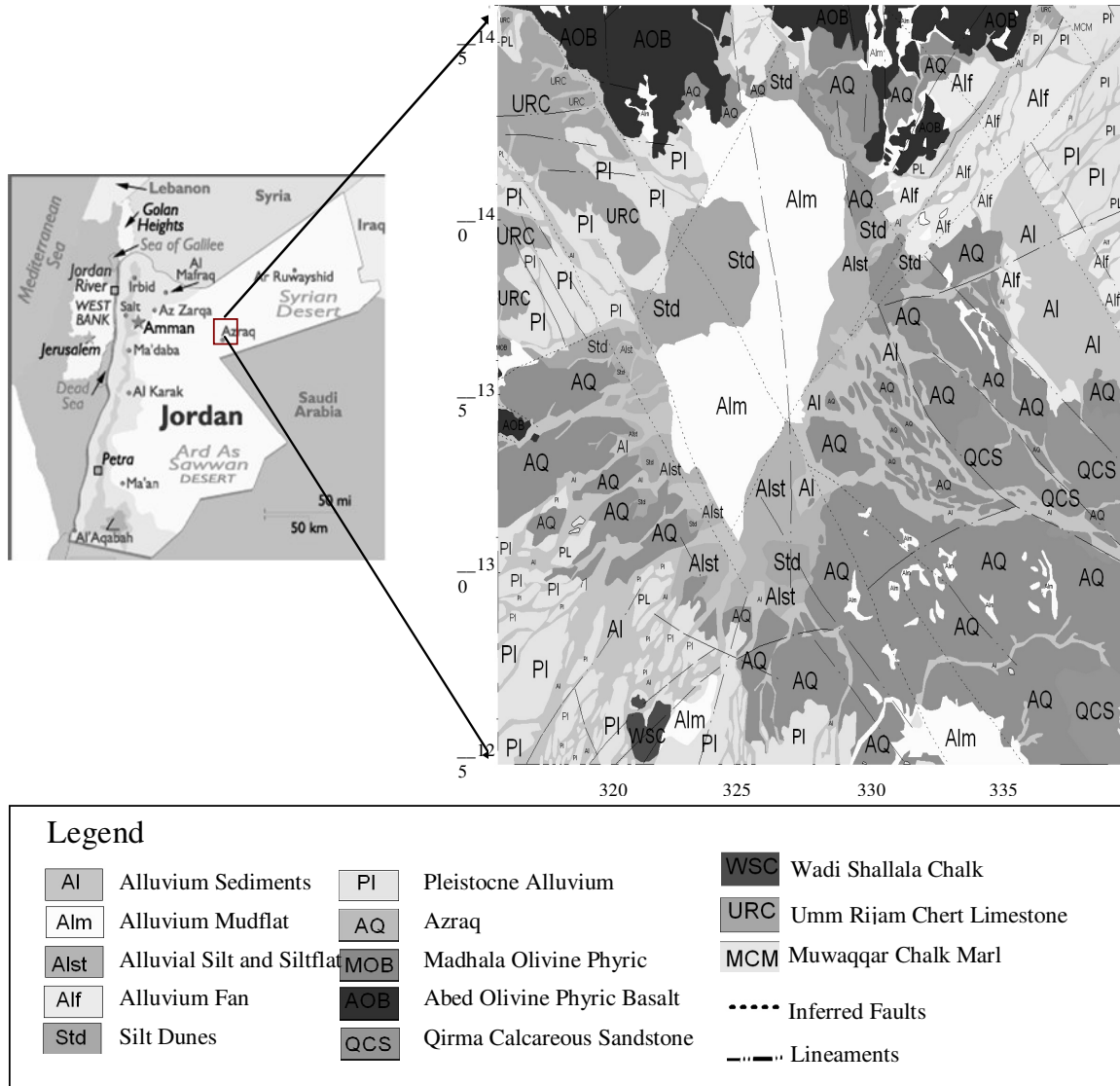


Figure 1. Geological map of the study area (modified after Ibrahim, 1996).

the same time, the directional effect illustrated by anisotropy is also determined using the cloud and azimuth variability within the semi-variograms.

Interpolation or estimation of values for points in an area not actually sampled was achieved by kriging (that is, a nearest-neighbor technique) in which values at locations close to the interpolation point are used to estimate the interpolation point value. Kriging uses the underlying spatial relationship in a data set (semivariogram) of the 16 nearest neighbors. Kriging was conducted based on regionalized variable theory and is superior to other means of interpolation because it provides an optimal interpolation estimate for a given coordinate location, as well as a variance estimate for the interpolation value. Since soil samples were taken to represent point values in the plot, at a specific time, punctual kriging was used in this study. Two-dimensional maps of clay contents data were constructed using contour levels to display the horizontal spatial distributions of clay within each depth interval.

Finally, kriged maps produced were used to calculate the clay reserve using advanced statistical and geostatistical methods through defining a query systems as function of polygon areas multiplied by the average estimate of the predicted clay content.

ESRI® ArcGIS Geostatistical Analyst (version 9.0) presents a comprehensive set of geoprocessing tools. It is an extension for advanced surface modeling using deterministic (non-geostatistical method) and geostatistical methods. In the other hand, Australia has encouraged the development of software solutions from ECSI. Development of gridding and contouring software for processing airborne geophysics used in mineral exploration led in the 1970's to the development of MINEX software for the coal mining industry. The MINEX is now recognized as a leader in seam or stratigraphic modeling and coal mine planning.

ArcMap and Minex were used to construct the kriging map and cross section in the Qa' Al-Azraq respectively.

## RESULTS AND DISCUSSIONS

### ArcMap software

Using the AcrMap software, the interpolation is usually more accurate since it is based on the geographical

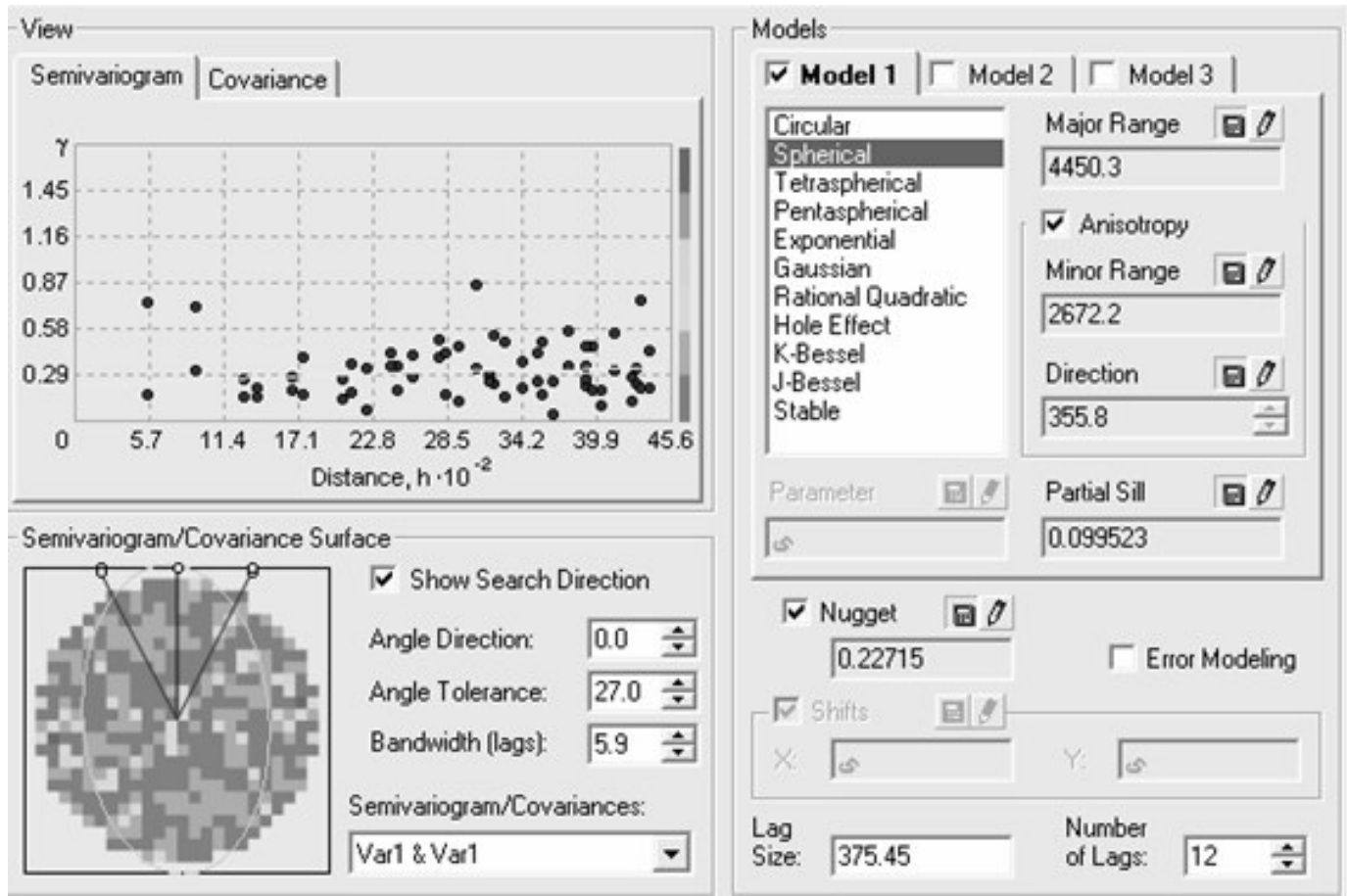


Figure 2. Semi-variogram model of the clay thickness.

distribution of the earth (actual spatial coordination). Prior to using the interpolation techniques, the data were explored using the exploratory spatial data analysis (ESDA) tools along the ArcMap software.

In semivariogram construction along the ArcMap software, the geostatistical analyst automatically calculates the optimum parameters (the major range, minor range, lag size, lag number and angle of direction), where dots on the semivariogram screen represents a pair of locations (Figure 2). The semivariogram surface below indicates the spatial directional effect illustrated by the anisotropy (ArcMap help, 2004).

Based on 27 degree tolerance, 12 numbers of lag and 0.37 km lag size, the empirical semi-variogram exhibits a spherical model. This model is one of the most commonly used where it shows progressive increase of semi-variance until some distance beyond which autocorrelation is zero. The theoretical best fit lines show semi-variogram models for many different directions. The major range (the range parameter for the major axis of variation) and minor range (the range parameter for the minor axis) were 4.4 and 2.6 km respectively. This means that the data becomes spatially independent after 4.4 km

along the major axis and 2.6 km along the minor axis. The nugget, representing the lowest variance due to variation between sample points at locations less the sampling distance or attributed to measurement errors, was estimated to be 0.22 while the partial sill (sill minus the nugget) were estimated to be 0.099 indicating a variation up to 0.299 at maximum scale for the whole data.

The error estimation for prediction can be detected using the regression function within ArcMap. Figure 3 below shows the scatter plot of predicted points (solid line) versus true values (black dashed line) where it is preferred to have a 1:1 line indicating a high coefficient of determination through the selected semivariance model. On the other hand, it is not always the case; within this analysis the slope was estimated to be less than one with a root mean square error (RMSE) of 13.81. To overcome this problem, it is a property of kriging that tends to under-predict large values and over-predict small values using the weighing functions (ArcMap help, 2004).

Figure 4 showed the final predicted Ordinary Kriging map for the clay deposits for the studied area. The maximum thickness predicted is nearly within the center of the studied area of about 50 m thick, and then decreases

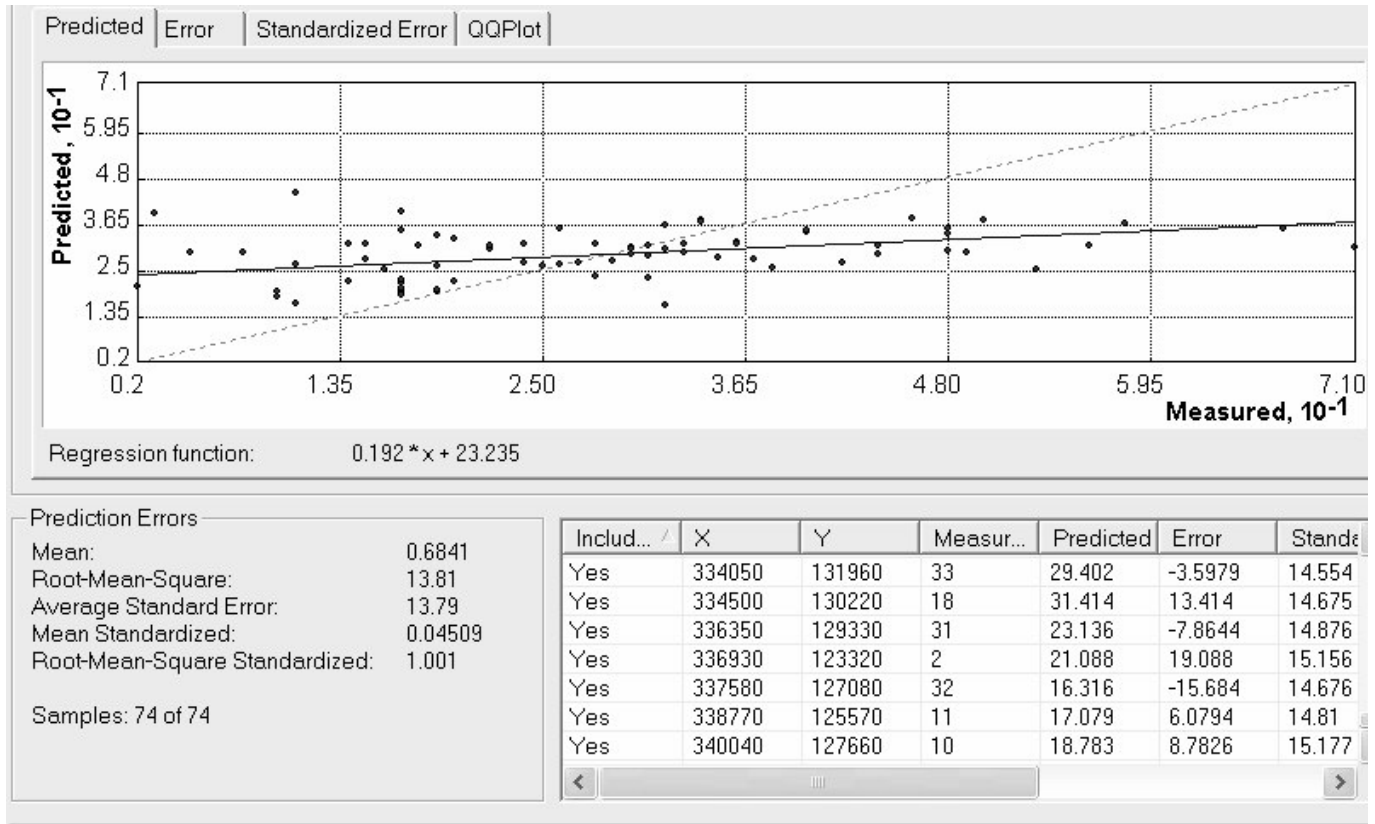


Figure 3. Prediction errors of the clay thickness.

systematically to reach about 13 m at the margins of the map. Structurally, faults have divided the studied area to two ponds; the first is bounded by four faults, Ar Rattami, Baqawiyya, Qaisyeh, and Al-Baida Faults, where the mean of the Kriging thickness is about 35 m. The other pond is bounded by Ar Rattami and Baqawiyya Faults where it is deeper and suitable to accumulate 40 m of clay deposits. Also, there is obviously a trend in the deposition of the clay deposit towards the northeast, as a result of the northeast faults. Ein Al-Baida area represents up thrown area as a result of Al-Baida Fault where it has a minimum clay thickness.

### Minex software

The software is based on gridding and modeling of the thickness of the sediments. Three Notepad files were considered as input database those are, collar, layer and lithology (MINEX manual, 1997). The files describe coordinates, sequences of layers, thickness and lithology. After modeling, the software correlates between boreholes to draw the cross sections. Two east-west cross sections (A and B) were built up (Figure 5). The distance between the two cross sections is approximately four kilometers.

The full description of the lithological sequences in cross sections in the studied area is shown in Table 1. Generally, the mean elevation of the studied area is about 500 m above sea level with a gentle dip towards the east where the thickness of the overburden increases. On the other hand, the clay deposits decrease gradually in the southwest direction. The effects of the Ar-Rattami Fault (northwest) and Baqawiyya Fault (northeast) are obvious in the eastern side of the cross sections.

The sections consist of clay, diatomite and interburden layers such as silt, sand and gypsum. The clay deposits are exposed near the surface at the eastern side of the section, while they gradually disappear gradually under the overburden deposits in the western side. In depth, they are separated to eight layers (CL1-CL8), where the mean thickness of these layers is approximately 60 m. Obviously, the tilting of the layers in the western side of the section is caused by Baqawiyya Fault. Due to that, a graben is formed, which is bounded between normal faults, where the sediments exhibit greater accumulations in this area.

Section (B) mainly represents the center of the study area and exhibits variations in the thickness of diatomite and clay due to faulting. The western side of the area (327-330 E) contains two major structures a graben and

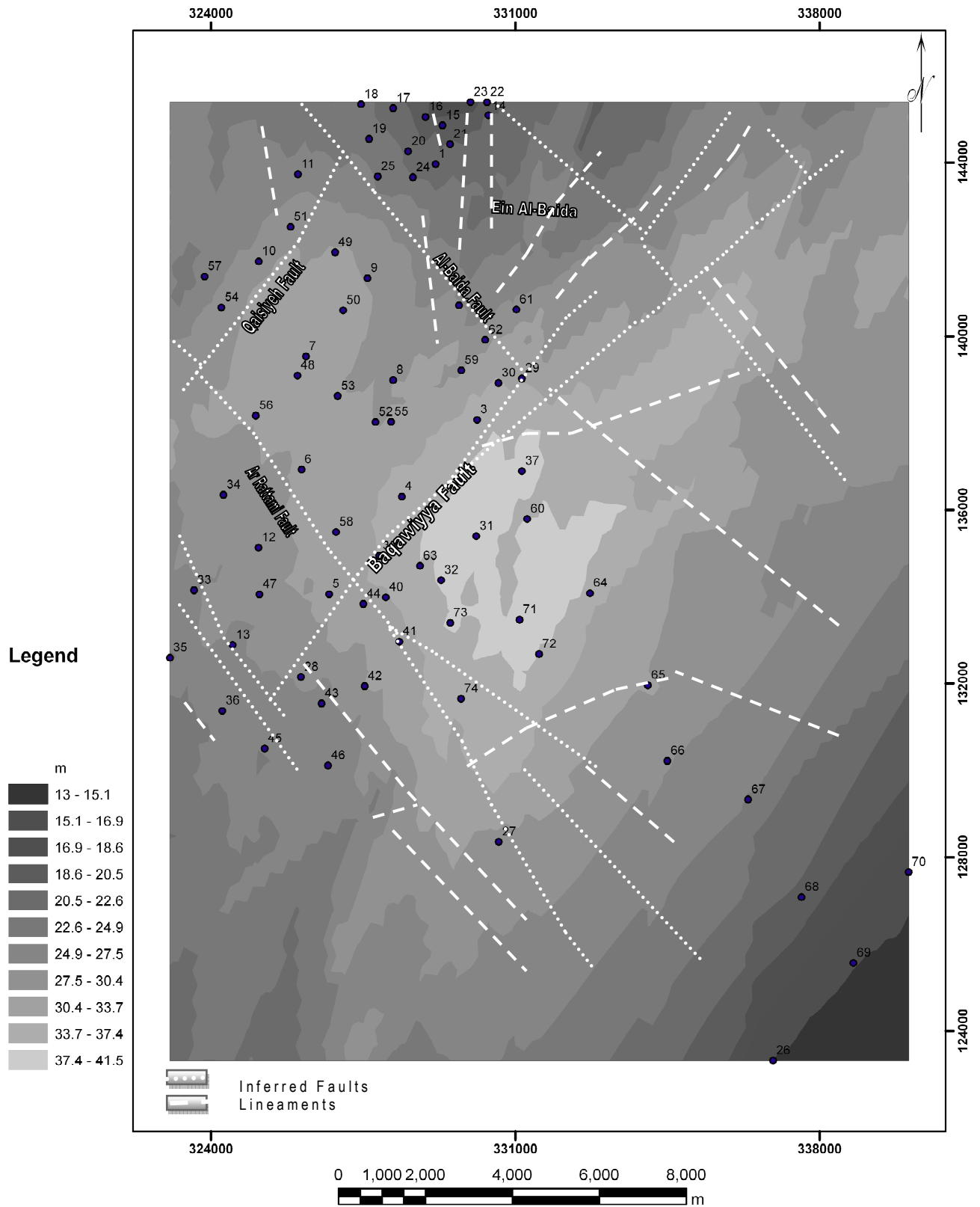


Figure 4. Ordinary Kriging map of the clay thickness.

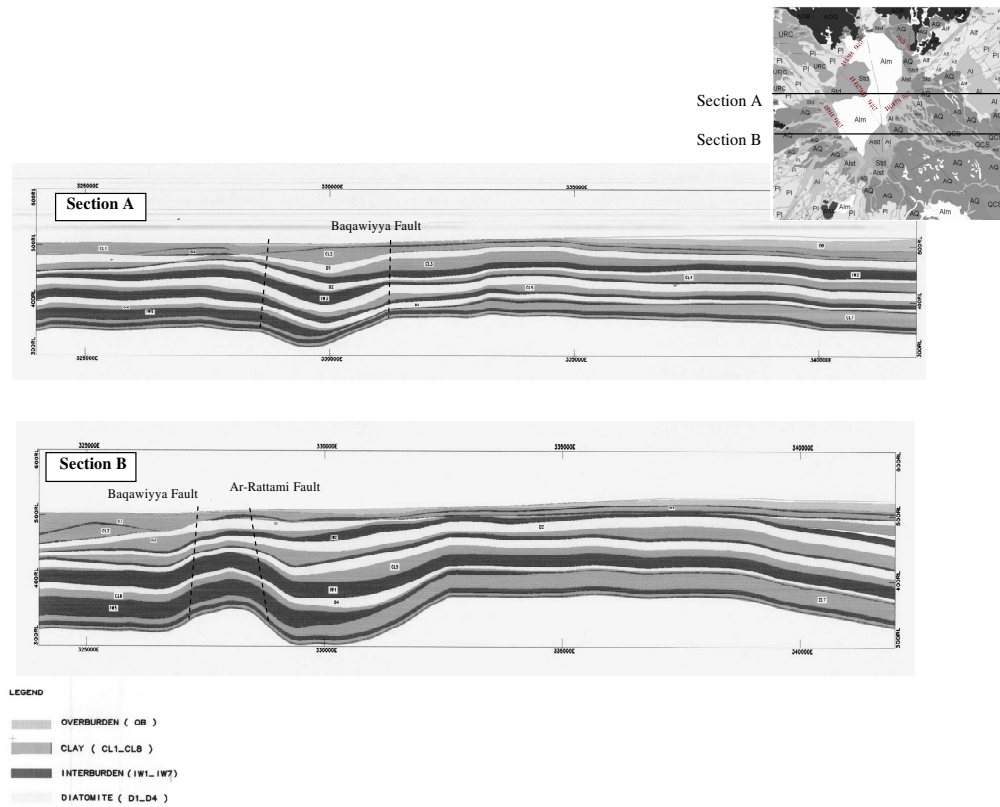


Figure 5. Cross sections in the study area, section A and section B.

a horst structure. Due to that, the thicknesses of the sediments have reached up to 200 m.

### ORE RESERVE ESTIMATION

The reserves were estimated depending on the thickness of the clay layers in each borehole. The reserve was estimated using the deterministic methods as Inverse Distance Method (IDM) and geostatistical method as Ordinary Kriging Method (OKM).

The MINEX software is actually based on IDM technique where the boreholes are posted and the selected area is specified by a polygon to determine the clay reserve as shown in Figure 6. In the other hand, the ArcMap software is based on OKM that is the most reliable method used for ore reserve estimation as the non-conventional method, which has been used widely for ore-reserve estimations because of its superior characteristics in relation to other methods. The method is actually define the spatial variance of the sample points allowing for better estimation of the reserve in accordance with the semivariance spatial dependence instead of simple weighing functions. The clay reserve estimation was based on the following equation:

$$\text{Reserve (m}^3\text{)} = \text{Kriging Mean value (m)} \times \text{Area (m}^2\text{)}$$

where the kriging mean value was estimated from the geospatial analysis and the area was evaluated from the Arc/map software.

As shown in the Table (2) the predicted clay reserves in the study area were 6.1 and 5.94 Billion Cubic Meter using MINEX and ArcMap, respectively. The MINEX and ArcMap are nearly similar to each other. According to field investigation, the clay deposit could be mined selectively where it is feasible for open cast mining due to low thickness and soft of overburden. Overall, the Inverse Distance Method and Kriging Method were significant to estimate any reserve, where the results are close to each other. However, the kriging values should be taken into consideration and could be used to estimate many other ores in Jordan.

Finally, it should be mentioned that what has been calculated is called inferred reserves. Later on and based on the industrial applications and characteristics of the ore, the recoverable reserves can be calculated.

### Conclusion

Clay thickness kriged map indicates a central concentration distribution of clay which coincides with the fact that the area represents the center of the ancient lacustrine. The variations in tones at the final krig map complies with the major local NW-SE and NE-SW fault

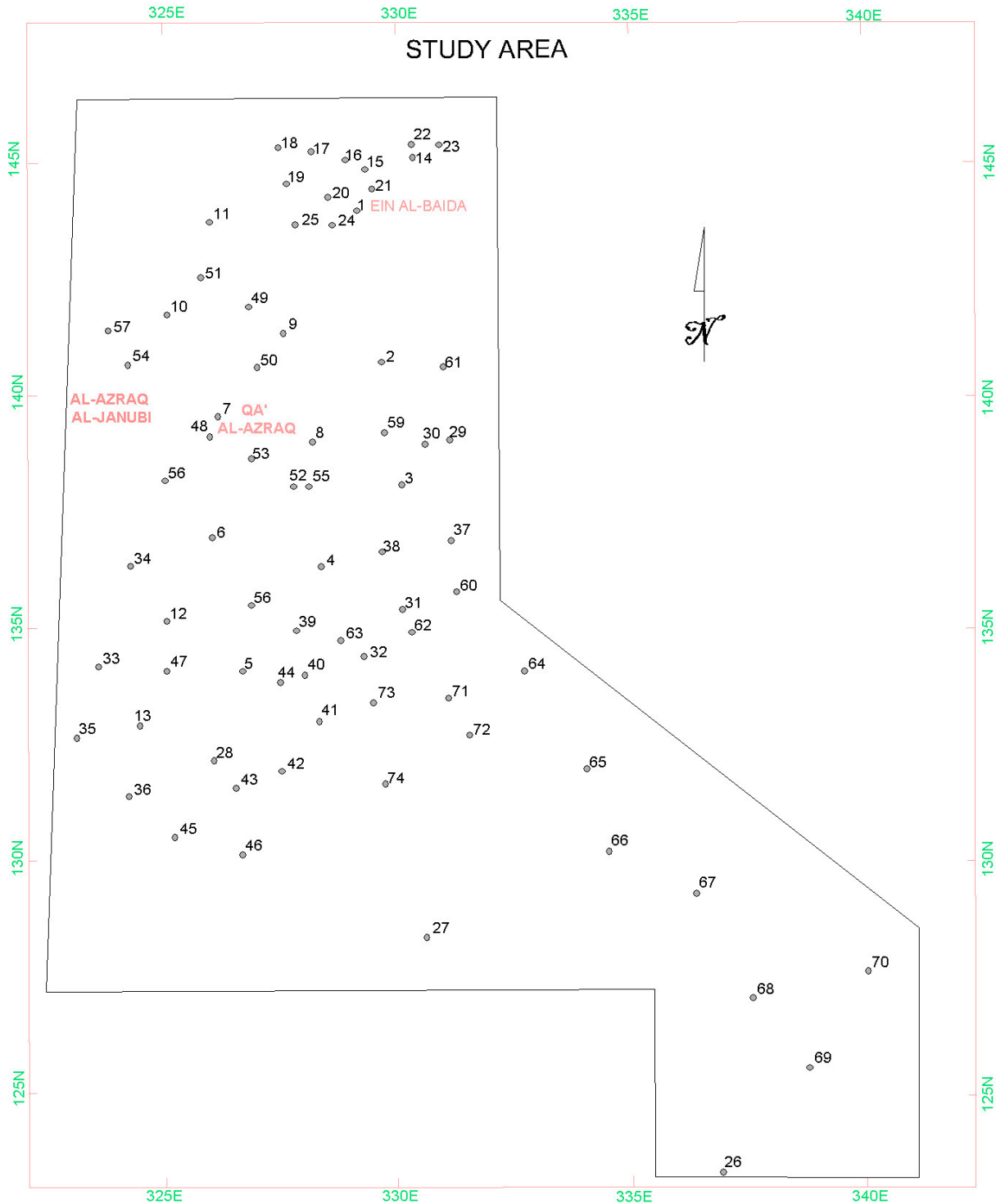


**Figure 6.** Location of boreholes and selected polygon.

systems where the center of the study area represents a pond structure allocated and bounded by the four faults (Ar Rattami, Baqawiyya, Qaisiyeh and Al-Baida). This situation explains the greatest thickness of the sediments presenting in the center of the study area.

The clay deposits were detected to be exposed near the surface at the eastern side of the first section, while they disappear gradually under the overburden deposits in the western side. The graben is formed between normal faults, here more sediment accumulations were

**Table 1.** Lithological sequence in the study area.

No.	Lithology	Symbol
1	Overburden	OB
2	Clay 1	CL1
3	Interburden	IW
4	Clay 2	CL2
5	Interburden 1	IW1
6	Diatomite 1	D1
7	Clay 3	CL3
8	Interburden 2	IW2
9	Diatomite 2	D2
10	Clay 4	CL4
11	Interburden 3	IW3
12	Diatomite 3	D3
13	Clay 5	CL5
14	Interburden 4	IW4
15	Diatomite 4	D4
16	Clay 6	CL6
17	Interburden 5	IW5
18	Clay 7	CL7
19	Interburden 6	IW6
20	Clay 8	CL8
21	Interburden 7	IW7
22	Clay 9	CL9

**Table 2.** Ore reserves estimations of the clay by Kriging method.

Polygon No.	Min. Value (m)	Max. Value (m)	Mean Value (m)	Area of Polygon (m <sup>2</sup> )	Reserve (m <sup>3</sup> )
1	11.52	18.8	15.16	10623397.63	161050708
2	18.8	24.38	21.59	15616616.78	337162756.4
3	24.38	28.65	26.515	28088662.99	744770899.2
4	28.65	31.91	30.28	44373773.99	1343637876
5	31.91	36.18	34.045	50697668.5	1726002124
6	36.18	41.76	38.97	23667317.49	922315362.7
7	41.76	49.04	45.4	15713315.51	713384524.3
Total				188,780,752.9	5,948,324,251

observed. On the other hand, the thickness of the clay deposits at southern side of the studied area has decreased where sandstone, conglomerate, and limestone layers started to appear underneath the clay.

Clay reserves were estimated depending on the thickness of the clay layers in each borehole using the deterministic methods as Inverse Distance Method (IDM) and geostatistical method as Ordinary Kriging Method (OKM). The predicted clay reserves at the study area were 6.1 and 5.94 Billion Cubic Meter using MINEX of IDM and ArcMap of OKM, respectively. The ordinary Kriging maps show thick sediments of clay beds intercalated with sand, silt and gypsum mainly in the center of Qa' Al-Azraq. The results of this study indicate that the area is a promising

future target for economic investment in the local raw materials.

#### ACKNOWLEDGEMENTS

The authors owe a great appreciation to the Natural Resource Authority for allowing us to evaluate the borehole data. Many thanks to Mr. Mohammed Al-Muhtaseb from Phosphate Company for his cooperation.

#### REFERENCES

Ala'li J, Abu Salah A (1993). Exploration for bentonite and other minerals in Azraq Depression. Natural Resources Authority, Jordan.

- Al-QinnaM (2003). Measuring and Modeling Soil Water and Solute Transport with Emphasis on Physical Mechanisms in Karst Topography, S594.A57, University of Arkansas, Fayetteville, AR, USA. Main, Special Collections, University of Arkansas, Fayetteville, AR, USA, unpubl. Ph.D. Thesis pp. 123-125.
- ArcMap help, Ibrahim KM (2004). ArcGIS Geostatistical Analyst (ESRI® version 9.0), ESRI Inc., USA.
- Clark I (1984). Practical Geostatistics. Elsevier applied science publishers. New York.
- Ibrahim KM (1996). The regional geology of Al-Azraq area, Bulletin No. 36, p. 56, Natural Resources Authority, Jordan.
- Issaks EH, Srivastava RM (1989). Applied geostatistics. Oxford University Press, New York.
- Khoury H (1980). Mineralogy and origin of Azraq clay deposits, Dirasat. 7: 21-31.
- MINEX manual (1997). ECS Mining software systems, version 4, Australia.
- Scott HD (2000). Soil physics: Agricultural and environmental applications. Iowa State University Press, Ames, Iowa.
- Selker JS, Keller CK, McCord JT (1999). Vadose zone processes. Lewis Publishers, CRC Press LLC, Florida.
- Sutherland RA, Van Kessel C, Pennock DJ (1991). Spatial variability of nitrogen-15 natural abundance. Soil Sci. Soc. Am J. 55: 1339-1347.
- Triantafilis J, Odeh IOA, McBratney AB (2001). Five geostatistical models to predict soil salinity from electromagnetic induction data across irrigated cotton. Soil Sci. Soc. Am. J. 65: 869-878.